© 2023. Published by The Company of Biologists Ltd | Disease Models & Mechanisms (2023) 16, dmm049783. doi:10.1242/dmm.049783

RESEARCH ARTICLE

Probing the pathogenicity of patient-derived variants of *MT-ATP6* in yeast

Emilia Baranowska[1], Katarzyna Niedzwiecka[1], Chiranjit Panja[1], Camille Charles[2], Alain Dautant[2], Jarosław Poznanski[1], Jean-Paul di Rago[2], Déborah Tribouillard-Tanvier[2,*] and Roza Kucharczyk[1,*]

ABSTRACT

The list of mitochondrial DNA (mtDNA) variants detected in individuals with neurodegenerative diseases is constantly growing. Evaluating their functional consequences and pathogenicity is not easy, especially when they are found in only a limited number of patients together with wild-type mtDNA (heteroplasmy). Owing to its amenability to mitochondrial genetic transformation and incapacity to stably maintain heteroplasmy, and the strong evolutionary conservation of the proteins encoded in mitochondria, *Saccharomyces cerevisiae* provides a convenient model to investigate the functional consequences of human mtDNA variants. We herein report the construction and energy-transducing properties of yeast models of eight *MT-ATP6* gene variants identified in patients with various disorders: m.8843T>C, m.8950G>A, m.9016A>G, m.9025G>A, m.9029A>G, m.9058A>G, m.9139G>A and m.9160T>C. Significant defect in growth dependent on respiration and deficits in ATP production were observed in yeast models of m.8950G>A, m.9025G>A and m.9029A>G, providing evidence of pathogenicity for these variants. Yeast models of the five other variants showed very mild, if any, effect on mitochondrial function, suggesting that the variants do not have, at least alone, the potential to compromise human health.

KEY WORDS: Mitochondrial diseases, ATP synthase, Yeast, Mitochondrial DNA mutation, MILS, LHON, mtDNA, *MT-ATP6*

INTRODUCTION

Mitochondrial diseases are a broad group of neuromuscular and metabolic disorders resulting from defects in oxidative phosphorylation, a process that provides cells with the energy-rich ATP molecule (Gorman et al., 2016). This process typically involves five protein complexes (I-V) embedded in the mitochondrial inner membrane that transfer electrons from food to oxygen coupled to production of ATP from ADP and inorganic phosphate (Saraste, 1999). Of the 90 subunits present in these complexes, 13 subunits are encoded by the mitochondrial genome [mitochondrial DNA (mtDNA)], while the others have a nuclear genetic origin; therefore, mutations in both genomes can cause these diseases.

Mutations of the mitochondrial genome are more frequent that those of the nuclear genome, possibly because of its exposure to mutagenic reactive oxygen species produced inside the organelle. Variations of this genome lead to mitochondrial diseases, and are also associated with common complex diseases like Alzheimer's disease, Parkinson's disease, Huntington diseases, diabetes, cancer, and a spectrum of nonspecific features like fatigue, deafness, multiple organ failure, schizophrenia and autism (El-Hattab et al., 2014; Hudson et al., 2014; Ju et al., 2014; Pfeffer and Chinnery, 2013; Wallace, 2010). With the advent of novel genomic sequencing methods, the list of such mutations is continuously expanding (Al-Kafaji et al., 2022; Wang et al., 2022). Evaluating their functional consequences and pathogenicity is not an easy task, especially when they are found in only a limited number of patients, sometimes a single individual, and when they coexist in cells and tissues with the wild-type mtDNA, which is referred to as heteroplasmy. The homoplasmic cybrid cell lines derived from patient cells are a reliable model for the evaluation of pathogenic effect of mtDNA variants. However, the nuclear background of the ρ^0 cell line generated to create the cybrid lines, often being the tumor cell line, contributes to conflicting findings (Wilkins et al., 2014). Recently, new mtDNA editing methods in mammalian cells have been developed; however, they are limited to specific nucleotide changes (Cho et al., 2022; Lei et al., 2022; Mok et al., 2020).

These difficulties led investigators to use the yeast *Saccharomyces cerevisiae* as a model to evaluate the consequences of mtDNA mutations found in patients. Owing to its good fermenting capacity, this unicellular fungus can efficiently survive mutations that inactivate oxidative phosphorylation, its mitochondrial genome can be modified [using a biolistic particle delivery system (Bonnefoy and Fox, 2001)], and heteroplasmy is highly unstable in this organism, making it possible to isolate strains homoplasmic for a given mtDNA mutation. Taking advantage of these attributes, we created yeast models of mutations in the *MT-ATP6* gene, encoding ATP synthase membrane subunit 6, with a proven or suspected pathogenicity (Kabala et al., 2014; Kucharczyk et al., 2019b, 2010, 2013, 2009a,b; Skoczen et al., 2018). All led to significant ATP production deficits in yeast mitochondria due to impairment of the functioning or assembly of the ATP synthase complex (Complex V) in which the protein encoded by *MT-ATP6* (subunit *a*) is essential for moving protons across the mitochondrial inner membrane coupled to ATP synthesis. Those mutations responsible for severe clinical phenotypes proved to affect dramatically the yeast ATP synthase, whereas those leading to milder diseases compromised oxidative phosphorylation in yeast

[1]Institute of Biochemistry and Biophysics, Polish Academy of Sciences, 02106 Warsaw, Poland. [2]University of Bordeaux, Centre National de la Recherche Scientifique, Institut de Biochimie et Génétique Cellulaires, UMR 5095, F-33000 Bordeaux, France.

*Authors for correspondence (roza@ibb.waw.pl; deborah.tribouillard-tanvier@ibgc.cnrs.fr)

E.B., 0000-0001-7349-1400; K.N., 0000-0002-9482-3918; C.P., 0000-0001-8235-1426; C.C., 0000-0002-2182-4928; A.D., 0000-0002-7145-278X; J.P., 0000-0003-2684-1775; J.-P.d.R., 0000-0002-3766-9002; D.T.-T., 0000-0002-2290-5375; R.K., 0000-0002-8712-7535

Handling Editor: Monkol Lek
Received 21 July 2022; Accepted 28 February 2023

Disease Models & Mechanisms (2023) 16, dmm049783. doi:10.1242/dmm.049783

mitochondria much less severely (Kucharczyk et al., 2009a,b), which validates the use of yeast as a model system to investigate the consequences of specific mutations in the human subunit *a*.

We here report the functional investigation, in yeast, of eight novel *MT-ATP6* variants detected recently in patients with various disorders: m.8843T>C, m.8950G>A, m.9016A>G, m.9025G>A, m.9029A>G, m.9058A>G, m.9139G>A and m.9160T>C. The results indicate that three of them (m.8950G>A, m.9025G>A and m.9029A>G) significantly compromise ATP synthase function, whereas the five others have very minor, if any, effect, suggesting that they do not have the potential, at least alone, to compromise human health.

RESULTS

Creation of yeast strains with equivalents of the human *MT-ATP6* gene mutations

The eight variants of the human *MT-ATP6* gene investigated in this study led to replacement of conserved residues of subunit *a*: p.I_{106}T (m.8843T>C), p.V_{142}I (m.8950G>A), p.I_{164}V (m.9016A>G), p.G_{167}S (m.9025G>A), p.H_{168}R (m.9029A>G), p.T_{178}A (m.9058A>G), p.A_{205}T (m.9139G>A) and p.Y_{212}H (m.9160T>C) (Table 1). The corresponding changes in the yeast subunit *a* (or Atp6) are, respectively, *a*I_{123}T, *a*V_{159}I, *a*I_{181}V, *a*G_{184}S, *a*H_{185}R, *a*T_{195}A, *a*A_{225}T and *a*Y_{232}H (see Fig. 5A for amino acid sequence alignments). These mutations were first introduced into the yeast *ATP6* gene carried by a plasmid (see Table 1 for the corresponding codon changes) and then delivered into the DNA-less (ρ^0) mitochondria of strain DFS160 with a biolistic system, giving the synthetic ρ^- *atp6*^{mut} strains (Fig. 1). These were crossed on glucose plates with layers of cells from strain MR10 (Rak et al., 2007b), in which the coding sequence of *ATP6* is replaced by *ARG8*^{m} [this is a mitochondrial version of a nuclear gene (*ARG8*) that encodes a mitochondrial protein (Arg8) involved in arginine biosynthesis (Steele et al., 1996)]. In ρ^- *atp6*^{mut}×MR10 (*atp6::ARG8*^{m}) zygotic cells, the variant of the *ATP6* gene can be integrated into a complete (ρ^+) mitochondrial genome by mtDNA recombination. The modified mitochondrial genome then segregates to homoplasmy in about a dozen mitotic divisions (without any selection pressure in rich 10% glucose), giving the strains ρ^+ *atp6*^{mut} used in the experiments described below. If the *atp6* mutation does not fully inactivate the ATP synthase, the mutant cells can be isolated by virtue of their ability to grow (even slowly) on respiratory carbon sources like glycerol. The eight ρ^- *atp6*^{mut}×MR10 crosses produced respiring clones, and, as expected, DNA sequencing confirmed that these carried the *atp6* mutations. Owing to the presence in DFS160 of the nuclear karyogamy delaying *kar1-1* mutation, the *atp6* mutations could be isolated in the haploid nuclear genetic background of MR10 (MR10 is derived from wild-type strain MR6) (Table S2).

Influence of the *atp6* mutations on the respiration-dependent growth of yeast

On solid media

As expected, the eight yeast *atp6* mutants grew well with fermentation of glucose, conditions under which ATP synthase function is not required (Fig. 2A). They grew quite well on respiratory carbon sources like glycerol, both at 28°C (the optimal temperature for yeast) and 36°C [at this temperature yeast mitochondrial function is partially compromised (Yamamura et al., 1988)]. This did not mean that the *atp6* mutations had no deleterious consequences. Indeed, large decreases in ATP synthase activity (~80%) are required to significantly affect the growth of yeast cells on non-fermentable substrates (Mukhopadhyay et al., 1994). However, with <80% ATP production deficits,

Table 1. *MT-ATP6* gene variants in patients and equivalent mutations in yeast

mtDNA mutation	Amino acid substitution	Number of cases	Disease/ syndrome	Biochemical data	Pathogenicity (MITOMAP/ ClinVar)	Pathogenicity score	Codon change in *ATP6* gene	Position in yeast Atp6p	References
m.8843T>C	p.I_{106}T	2	Schizophrenia	n.d.	R/benign	0.642	ATT>ACT	I_{123}T	Ganetzky et al., 2019; Ueno et al., 2009
m.8950G>A	p.V_{142}I	2	LHON plus dystonia/ Leigh-like syndrome	n.d.	R/benign	0.439	GTT>ATT	V_{159}I	Abu-Amero and Bosley, 2005; Brautbar et al., 2008
m.9016A>G	p.I_{164}V	2	LHON	n.d.	R/likely benign	0.621	ATC>GTC	I_{181}V	Povalko et al., 2005
m.9025G>A	p.G_{167}S	3	MILS	n.d.	R/benign	0.86	GGT>AGT	G_{184}S	Lopez-Gallardo et al., 2014
m.9029A>G	p.H_{168}R	1	LHON-like	Reduced ATP synthase activity, higher ROS production	R/uncertain significance	0.827	CAT>AGA	H_{185}R	Lopez-Gallardo et al., 2014
m.9058A>G	p.T_{178}A	2	LVHT	n.d.	R/benign	0.209	CTA>GCA	T_{195}A	Ganetzky et al., 2019; Tang et al., 2010
m.9139G>A	p.A_{205}T	19*	LHON	n.d.	R/benign	0.65	GCT>ACT	A_{225}T	La Morgia et al., 2008
m.9160T>C	p.Y_{212}H	1	Schizophrenia	n.d.	R/uncertain significance	0.69	TAT>CAT	Y_{232}H	Sequeira et al., 2015

LHON, Leber hereditary optic neuropathy; LVHT, left ventricular hypertrabeculation syndrome; MILS, maternally inherited Leigh syndrome; mtDNA, mitochondrial DNA; n.d., not determined; R, reported; ROS, reactive oxygen species. *Members of one family. A pathogenicity score >0.7 was considered a high pathogenicity score, according to Pereira et al. (2011).

Disease Models & Mechanisms (2023) 16, dmm049783. doi:10.1242/dmm.049783

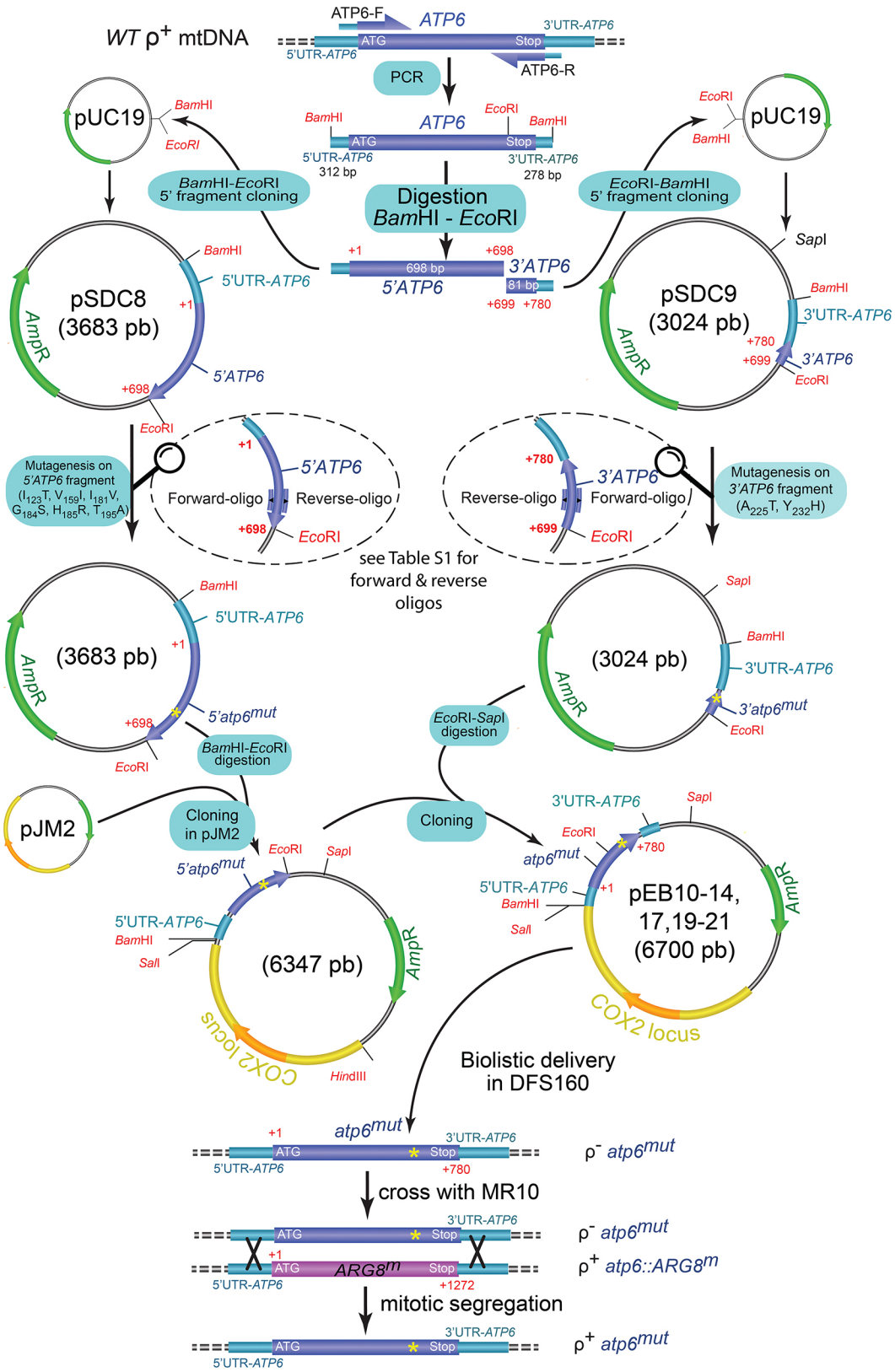

Fig. 1. Schema of the procedure used to create the ρ⁺ *atp6*^{mut} strains. The mutations (*atp6*^{mut}) are first introduced in one of two plasmids carrying a 5′ (pSDC8) or 3′ (pSDC9) fragment of the yeast *ATP6* gene. The 5′ fragment (mutated or non-mutated) is cleaved and cloned in pJM2 and is then joined with the 3′ fragment (mutated or non-mutated) using the indicated restriction enzymes to reconstitute the entire *ATP6* gene with the *atp6*^{mut} mutation. The resulting plasmids (pEB) are delivered with a biolistic system in the DNA-less (ρ^0) mitochondria of strain DFS160, giving the synthetic strains ρ^- atp6^{mut}. These are crossed with a strain (MR10) in which the coding sequence of *ATP6* is replaced by *ARG8*^{m}. In the mated cells, *ARG8*^{m} is replaced by the mutated *atp6* gene by DNA recombination, and, after a dozen mitotic divisions, cells homoplasmic for the *atp6*^{mut} mutation in a complete (ρ^+) mtDNA emerge.

Disease Models & Mechanisms (2023) 16, dmm049783. doi:10.1242/dmm.049783

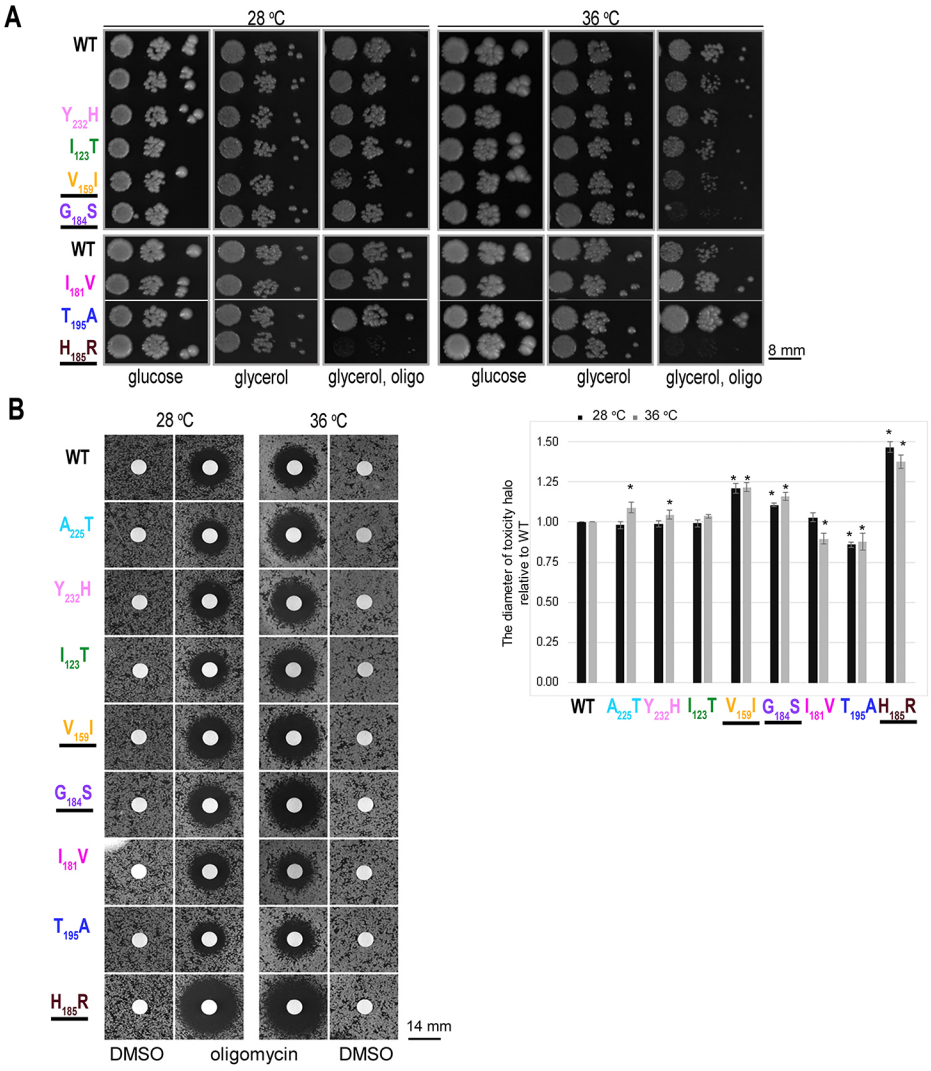

Fig. 2. Influence of *atp6* mutations on the respiration-dependent growth of yeast. (A) Fresh glucose cultures of the *atp6* mutants and wild-type yeast were serially diluted and spotted on rich glucose and glycerol plates supplemented or not with oligomycin (0.5 µg/ml) and incubated at 28°C or 36°C. The glucose and glycerol plates were photographed after 3 days of incubation, while the glycerol plates supplemented with oligomycin were incubated for one more day before being photographed. Gray borders demarcate strains grown on the same plate. Strains for which growth is different from that of the control strain are underlined. WT, wild type. (B) Cells from the indicated strains were spread as dense layers onto rich glycerol solid media and then exposed to sterile filters spotted with 20 nmol oligomycin and DMSO as a negative control (solvent). The plates were scanned after 4 days of incubation at 28°C and 36°C. The diameters of the halos of growth inhibition (in % of WT) are reported in the shown histograms. **P*<0.001 (unpaired two-tailed Student's *t*-test). (C) Growth in liquid glucose and glycerol media. The cultures were inoculated with cells freshly grown in glucose and monitored with a Bioscreen CTM system. **P*<0.05 (unpaired two-tailed Student's *t*-test). The shown data are representative of three independent experiments. OD, optical density.

Disease Models & Mechanisms (2023) 16, dmm049783. doi:10.1242/dmm.049783

respiration-dependent growth of yeast becomes more sensitive to oligomycin, a specific inhibitor of ATP synthase, because less of this drug is then needed to reach the ATP synthase activity threshold (Kucharczyk et al., 2010). As shown in Fig. 2A, at a concentration of oligomycin (0.5 µg/ml) that had no effect on wild-type yeast, the respiration-dependent growth of two mutants (aH$_{185}$R and aG$_{184}$S) was fully inhibited at 28°C and 36°C (aH$_{185}$R), or mainly at 36°C (aG$_{184}$S), growth of aV$_{159}$I was slightly inhibited, and growth of the five other mutants was preserved. The sensitivity of growth to oligomycin was further quantified. Cells were spread as a dense layer on glycerol medium and then exposed to a drop of oligomycin deposited on a sterile filter (Fig. 2B). Oligomycin diffuses in the growth medium, which results in the establishment of a continuous gradient around the filters. Growth is inhibited until a certain drug concentration, which manifests as a halo of no growth around the filter, the diameter of which can be measured. The halos of growth inhibition had a much higher diameter for aH$_{185}$R, aG$_{184}$S and aV$_{159}$I versus that of wild-type yeast (Fig. 2B), further indicating that these three substitutions have detrimental effects on ATP synthase.

In liquid media

To better appreciate the influence of the *atp6* mutations on the growth of yeast, we followed changes in cellular density over time in rich glucose and glycerol liquid media, at 28°C and 36°C. In liquid glucose, the cells first multiplied rapidly by fermentation and then more slowly by respiring the ethanol that resulted from glucose fermentation in the rapid growth phase. Although there was no obvious difference between the mutants and the wild type as long as glucose was present (Fig. 2C), the aH$_{185}$R mutant divided less rapidly than the other strains in the ethanol-dependent growth phase at 36°C. Consistently, this mutant showed a significantly reduced efficiency to grow in liquid glycerol (another substrate that, like ethanol, cannot be fermented), whereas much smaller differences were observed with the seven other mutants relative to wild-type yeast (Fig. 2C).

Influence of the *atp6* mutations on the assembly/stability of ATP synthase

The influence of the *atp6* mutations on ATP synthase assembly/stability was evaluated by blue native (BN)-polyacrylamide gel electrophoresis (PAGE) of mitochondrial digitonin extracts prepared from cells grown in rich galactose medium (YPGalA). In samples from the wild type, using antibodies specific to its subunits *a* and Atp2 (β-F_1), ATP synthase was detected mainly as dimers and monomers, with only trace amounts of free F_1 particles not associated with F$_O$ (Fig. 3A). A similar pattern was observed in samples from the eight *atp6* mutants. There was no important difference in the levels of ATP synthase subunits Atp2, Atp7 (a subunit of the peripheral arm of ATP synthase) and Atp6 in total cellular protein extracts separated in denaturing gels (Fig. 3B). About a 18-25% decrease in the amount of the aI$_{123}$T subunit was associated with increased amounts of mtDNA-deficient cells in cultures of these mutant cells (see Table 2). These data indicate that the mutations had little, if any, effect on the assembly/stability of subunit *a* within ATP synthase.

Respiration and ATP synthesis activities

The influence of the *atp6* mutations on oxygen consumption and ATP synthesis was investigated in intact (osmotically protected) mitochondria isolated from cells grown in galactose-rich medium at 28°C and 36°C. Oxygen consumption was measured using NADH as an electron donor. In yeast, in which there is no Complex I,

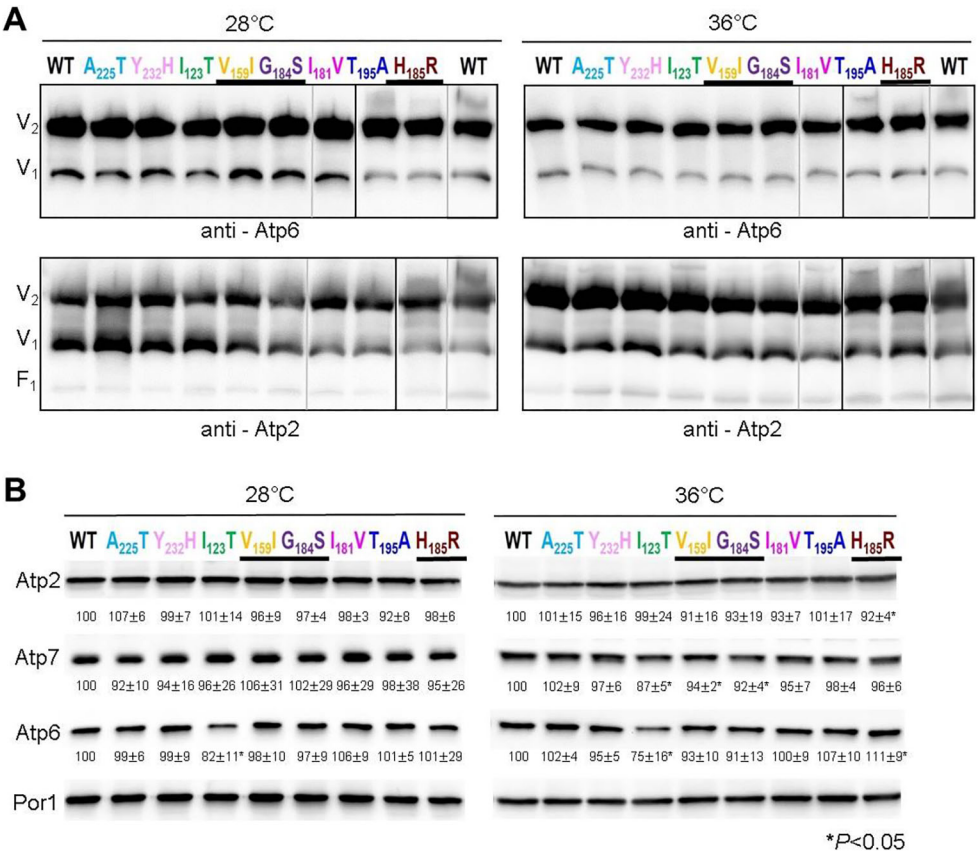

Fig. 3. Influence of *atp6* mutations on ATP synthase assembly/stability. (A) Mitochondria isolated from the *atp6* mutants and wild-type yeast grown at the indicated temperature were solubilized with digitonin (1.5 g/g protein), and 200 µg of proteins were separated in BN gels containing a 3-12% polyacrylamide gradient. The proteins were transferred to a PVDF membrane and probed with antibodies against subunits *a* (Atp6) and Atp2 (β-F_1) of ATP synthase. The immunological signals corresponding to dimers (V_2) and monomers (V_1) of ATP synthase and free F_1 particles are indicated. Lanes from the same gel are demarcated by black borders, and the control lane (WT) from each gel is shown. Gray lines separate lanes that were not loaded side by side. (B) Total cellular protein extracts were separated by SDS-PAGE and then transferred to a nitrocellulose membrane and probed with antibodies against the indicated proteins. The intensity of bands was calculated using ImageJ, normalized to porin, and the differences are expressed as a percentage relative to the control strain. *P*-values and s.e.m. were calculated from three independent experiments. **P*<0.05 (unpaired two-tailed Student's *t*-test).

Disease Models & Mechanisms (2023) 16, dmm049783. doi:10.1242/dmm.049783

Table 2. Mitochondrial respiration and ATP synthesis activities

			Oxygen consumption (nmol O_2 min^{-1} mg^{-1})				Oli^S ATP synthesis (nmol Pi min^{-1} mg^{-1})		
				NADH+ADP (state 3)					
Strain	Temperature	% ρ^-/ρ^0	NADH (state 4)		% WT	RCR		% WT	P/O
WT	28°C	2±2	579±71	1232±130	100±10	2.19±0.49	1070±95	100±9	0.88±0.17
$A_{225}T$	28°C	2±2.6	429±31*	989±87*	80±7	2.33±0.37	942±43	88±4	0.96±0.13
$Y_{232}H$	28°C	1.3±1.5	358±27*	1156±34	93±3	3.24±0.34	924±141	86±15	0.80±0.15
$I_{123}T$	28°C	2.5±3.5	464±91	911±25*	74±2	2.09±0.41	947±51	88±5	1.03±0.09
$V_{159}I$	28°C	1.5±0.7	451±11*	930±92*	76±7	2.06±0.2	695±21*	65±3	0.75±0.05
$G_{184}S$	28°C	2.8±4	510±22	1019±31*	82±2	1.99±0.01	725±24*	68±2	0.71±0.05
$I_{181}V$	28°C	3±1.7	442±82	1094±35	89±3	2.57±0.55	927±94	87±10	0.85±0.11
$T_{195}A$	28°C	3±4	480±71	987±108	80±9	2.13±0.54	976±132	91±13	1.01±0.25
$H_{185}R$	28°C	6.5±2	439±30*	907±75*	74±6	2.08±0.31	798±80*	75±10	0.89±0.16
WT	36°C	37±3	295±29	631±62	100±9	2.18±0.42	662±104	100±14	1.07±0.27
$A_{225}T$	36°C	31±2	254±2	580±35	92±5	2.28±0.15	570±74	86±11	0.99±0.19
$Y_{232}H$	36°C	30±3	281±8	696±57	110±9	2.48±0.27	592±9	89±2	0.88±0.06
$I_{123}T$	36°C	51±6*	265±1	636±58	101±9	2.40±0.23	546±106	82±17	0.87±0.25
$V_{159}I$	36°C	41±6	234±16*	544±8*	86±1	2.28±0.15	382±30*	58±8	0.72±0.04
$G_{184}S$	36°C	42±8	246±7*	630±70	100±11	2.56±0.36	341±46*	51±11	0.55±0.14
$I_{181}V$	36°C	28±7	261±3	583±47	92±7	2.24±0.22	704±73	106±9	1.22±0.23
$T_{195}A$	36°C	45±7	288±7	635±6	100±1	2.19±0.07	526±77	80±10	0.82±0.13
$H_{185}R$	36°C	31±14	160±3*	351±68*	56±11	2.20±0.47	404±72*	61±15	1.23±0.31

Mitochondria were isolated from wild-type and mutant strains grown for five to six generations in YPGalA at 28°C or 36°C. '% ρ^-/ρ^0' is the percentage of cells lacking complete mtDNA in cultures. Reaction mixes for assays contained 0.075 mg/ml protein, 4 mM NADH, 150 (for respiration assays) or 750 (for ATP synthesis) µM ADP, 3 µg/ml oligomycin (Oli). Oli^S, oligomycin sensitive; P/O, ATP made per O atom reduced; RCR, respiratory control ratio; WT, wild type. The values reported are averages of triplicate assays±s.d. *P<0.05 (unpaired two-tailed Student's t-test). Strains for which activities are statistically different from those of the control strain are underlined.

electrons from NADH added to mitochondria are transferred to ubiquinone without any proton pumping by dehydrogenases (Nde1/2) located at the external surface of the inner membrane and are next transferred to oxygen, as in humans, by the proton-translocating Complexes III (bc_1) and IV (aa_3) (Michel, 1998; Schultz and Chan, 2001; Berry et al., 2000). With the addition of NADH alone (basal or state 4 respiration), the rate of electron transfer is mainly controlled by the passive permeability to protons of the inner membrane. With mutations that induce proton leaks through the F_O, state 4 respiration will increase (Duvezin-Caubet et al., 2006). None of the investigated mutations stimulated state 4 respiration (Table 2), indicating the absence of such proton leaks. After a subsequent addition of ADP (state 3 respiration), the rate of electron transfer to oxygen is normally about twice stimulated to maintain across the membrane the proton gradient that is now used by the ATP synthase to produce ATP (Hinkle, 2005). Consistent with the quite good growth of the mutants on glycerol (Fig. 2A), their mitochondria responded quite well to the addition of ADP. However, a significant decrease in the rate of oxygen consumption, up to 55% (depending on the growth temperature), was observed for aH$_{185}$R relative to that in wild-type yeast (Table 2). Consistently, the mitochondria from this mutant showed a similarly reduced rate of ATP synthesis. The reduced capacity of this mutant to transfer electrons to oxygen is a secondary consequence of a defect in ATP synthase and not the inverse, as was observed and discussed in previous studies (Kabala et al., 2014; Kucharczyk et al., 2019b, 2013, 2009b). Oxygen consumption at state 3 was reduced in mitochondria of aG$_{184}$S and aV$_{159}$I by ∼15-24%, while the rate of ATP synthesis was reduced by ∼30-51%, with statistical significance. The compromised ability of the aH$_{185}$R, aG$_{184}$S and aV$_{159}$I cells to produce ATP in mitochondria corroborates their higher sensitivity to oligomycin when grown from non-fermentable substrates (Fig. 2B). The differences in ATP synthesis seen with the five other mutations investigated in this study were not statistically significant (Table 2), indicating that they had only minor, if any, detrimental effects on ATP synthase.

We further evaluated the influence of substitutions in subunit a on oxidative phosphorylation by monitoring changes in the mitochondrial transmembrane potential (ΔΨ). In a first series of experiments (Fig. 4; Fig. S1A), we tested the capacity of ADP to induce ΔΨ in ethanol-energized mitochondria due to proton re-entry through the F_1F_O-ATP synthase, followed by a total collapse of the membrane potential with further additions of potassium cyanide (KCN) and carbonyl cyanide m-chlorophenylhydrazone (CCCP). Mitochondria from all strains responded similarly to the control mitochondria except those from aH$_{185}$R cells grown at elevated temperature, which needed more time to re-establish the potential after addition of ADP. We next investigated the ability of ATP synthase to rebuild the ΔΨ when working in the reverse mode (Fig. S1B). The mitochondria were energized by ethanol, the resulting ΔΨ was collapsed with KCN, and ATP was then rapidly added. In these conditions, the natural F_1 inhibitor protein IF1 is released from F_1 and does not re-bind (Venard et al., 2003). In mitochondria of all strains, ATP addition induced a large and stable ΔΨ that was fully reversed by oligomycin.

DISCUSSION

It is in the *MT-ATP6* gene encoding the subunit a of ATP synthase that the first pathogenic mutation of mtDNA, m.8993T>G, was identified >30 years ago (Holt et al., 1990). Since then, dozens of mutations of this gene were detected in patients with various neuromuscular diseases (Dautant et al., 2018). With the recent advent of complete structures of ATP synthase from various mitochondrial origins (Guo et al., 2017; Hahn et al., 2016; Sobti et al., 2020; Spikes et al., 2020), we better understand the mechanism of proton transport through the F_O domain of the enzyme, and we can analyze how amino acid substitutions disrupt the functioning of the enzyme. The subunit a and a ring of identical

Disease Models & Mechanisms (2023) 16, dmm049783. doi:10.1242/dmm.049783

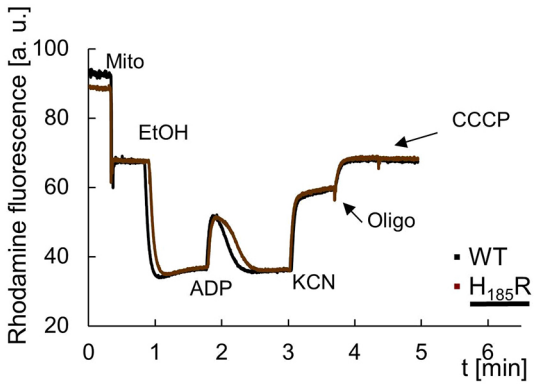

Fig. 4. Variations in mitochondrial inner membrane potential in *a*H$_{185}$R mitochondria isolated from cells grown at 36°C. The tracings show how the mitochondria responded to externally added ADP. The additions were 75 µM ADP, 0.5 µg/ml Rhodamine 123, 75 µg/ml mitochondrial proteins (Mito), 10 µl ethanol (EtOH), 2 mM potassium cyanide (KCN), 4 µg/ml oligomycin (Oligo) and 4 µM carbonyl cyanide-m-chlorophenyl hydrazone (CCCP). The shown tracings are representative of three biological repetitions. a.u., arbitrary units.

subunits *c* (eight in humans, ten in yeast) are responsible for the transport of protons across the membrane domain (F_O) of ATP synthase (Fig. 5). Two hydrophilic pockets on the external (*p*) and internal (*n*) sides of the inner membrane allowing access to the contact zone between the *c*-ring and subunit *a* enable the transfer of protons from the intermembrane space of mitochondria to an acidic residue in subunit *c* (*c*E$_{59}$ in yeast) and their release in the mitochondrial matrix after an almost complete rotation of the *c*-ring (Guo et al., 2017). The *p*- and *n*-side pockets are separated by a plug of hydrophobic residues of subunit *a* near the middle of the membrane, and close to it, in front of *c*E$_{59}$, is a positively charged arginine residue (*a*R$_{176}$ in yeast) that is essential for moving protons through the F_O (Guo et al., 2017). Of the eight mutations herein investigated, two *a*H$_{185}$R and *a*G$_{184}$S that significantly impacted ATP synthase function are within the *p*-pocket. It can be inferred from mutagenesis studies in *Escherichia coli* (Cain and Simoni, 1988; Lightowlers et al., 1988), and atomic structures of bacterial and mitochondrial ATP synthases (Guo et al., 2017; Sobti et al., 2020; Srivastava et al., 2018), that the *a*H$_{185}$ residue of yeast subunit *a* is most likely involved in F_O-mediated proton transfer in concert with a nearby glutamate residue (*a*E$_{223}$ in yeast), owing to the ability of these two residues to exchange protons (Fig. 5C). Although it can also exchange protons owing to its guanidinium group, the side-chain of *a*R$_{185}$ is, according to our structural modeling analyses, more distantly located from *a*E$_{223}$ than the imidazole group of *a*H$_{185}$. Additionally, *a*R$_{185}$ has the ability to make hydrogen bonds with a glutamine residue (*a*Q$_5$) located near the N-terminal end of subunit *a* (Fig. 5C). Therefore, the replacement of histidine in position 185 with arginine will impair the function of *a*E$_{223}$ in the transport of protons. The lack of a side chain at position 184 (owing to its occupation by a glycine residue) is presumably important to avoid steric hindrance between *a*H$_{185}$ and *a*E$_{223}$ (Fig. 5C). In our structural analyses, the hydroxyl group of the serine side-chain in position 184 can make a hydrogen bond with *a*E$_{223}$ and thereby compromise its proton-conduction function within the *p*-pocket. Although the six other *MT-ATP6* gene variants herein investigated lead to replacement of well-conserved subunit *a* residues (*a*I$_{123}$T, *a*V$_{159}$I, *a*I$_{181}$V, *a*T$_{195}$A, *a*A$_{225}$T and *a*Y$_{232}$H, in the yeast protein), these are in positions remote from the regions at the *a*/*c* interface that are critical for F_O-mediated proton transport (Fig. 5B,C). These changes do not induce steric or charge hindrance in their proximal environment.

If the structural analysis considerably helps making predictions on how discrete structural changes in subunit *a* may influence the stability/activity of ATP synthase, and hence human health, a genetically approachable model system is required to test such predictions. The yeast *S. cerevisiae* is a particularly convenient system for investigations of substitutions in mitochondrially encoded subunits that are highly conserved, like subunit *a* of ATP synthase (Fig. 5A). Its mitochondrial genome can be manipulated, and heteroplasmy is highly unstable in this organism. Taking advantage of these unique attributes, we were able to define how ten *ATP6* mutations known to be pathogenic affect the ATP synthase (Ding et al., 2020; Kabala et al., 2014; Kucharczyk et al., 2019a,b, 2010, 2013, 2009a,b,c; Skoczen et al., 2018; Su et al., 2020, 2021). In this study, we investigated, in yeast, eight additional missense *MT-ATP6* mutations recently identified in patients, for which there is little understanding of how these mutations cause disease.

Four of these mutations (m.8950G>A, m.9016A>G, m.9029A>G and m.9139G>A) were found in a very small number of patients (one or two individuals only) presenting with clinical features typical of Leber hereditary optic neuropathy (LHON), a disease characterized by optic nerve degeneration and loss of vision (Finsterer et al., 2018). Thus far, LHON-causing mutations were mostly located in the mitochondrial MT-ND genes encoding subunits of Complex I. Although they affect highly conserved residues of subunit *a*, equivalents of m.9016A>G and m.9139G>A had no obvious detrimental effects on the activity and assembly/stability of the yeast ATP synthase, which casts in doubt their potential, at least alone, to impair vision. Consistently, the amino acid replacements they induce are not in regions of subunit *a* known to be critical for moving protons across the membrane domain of ATP synthase (Fig. 5). The health problems of the individuals with m.9016A>G and m.9139G>A are thus likely to be caused by the primary mtDNA variants leading to LHON, also found in those two patients: m.14484T>C mutation in *MT-ND6* and m.11778G>A mutation in *MT-ND4* genes, respectively (La Morgia et al., 2008; Povalko et al., 2005). We cannot rule out, however, that they might have some detrimental effects if combined with other mutations in nuclear DNA or mtDNA that affect the process of oxidative phosphorylation, as was documented for a number of other mutations of the human mtDNA (Ban et al., 2008; McManus et al., 2019). In contrast, the m.8950G>A variant was found in two unrelated patients: alone in a female with LHON plus dystonia (Abu-Amero and Bosley, 2005) and in combination with the m.13513G>A leading to p.D$_{393}$N substitution in the ND5 subunit of the respiratory chain complex I in an individual with Leigh-like syndrome (Brautbar et al., 2008). The family history and biochemical data from patients cells are missing; thus, it is unclear why this mutation was classified as benign in the ClinVar database (Table 1). Substitution of *a*V159 into I in yeast Atp6 protein inhibited the growth of yeast cells on respiratory medium in the presence of oligomycin and decreased the ATP production rate by ∼35%. Our data indicate that this mutation alone may have led to LHON in the patient described in Abu-Amero and Bosley (2005) and could have aggravated the severity of Leigh disease in the patient described in Brautbar et al. (2008), but more patient data are needed to classify this variant as pathogenic.

Regarding the fourth *MT-ATP6* variant (m.9029A>G), detected in an atypical LHON patient (with progressive loss of vision over 4 years) and in a second patient diagnosed with mitochondrial disorder, there is some evidence that it might have detrimental effects on mitochondrial function and was therefore suspected to be

Disease Models & Mechanisms (2023) 16, dmm049783. doi:10.1242/dmm.049783

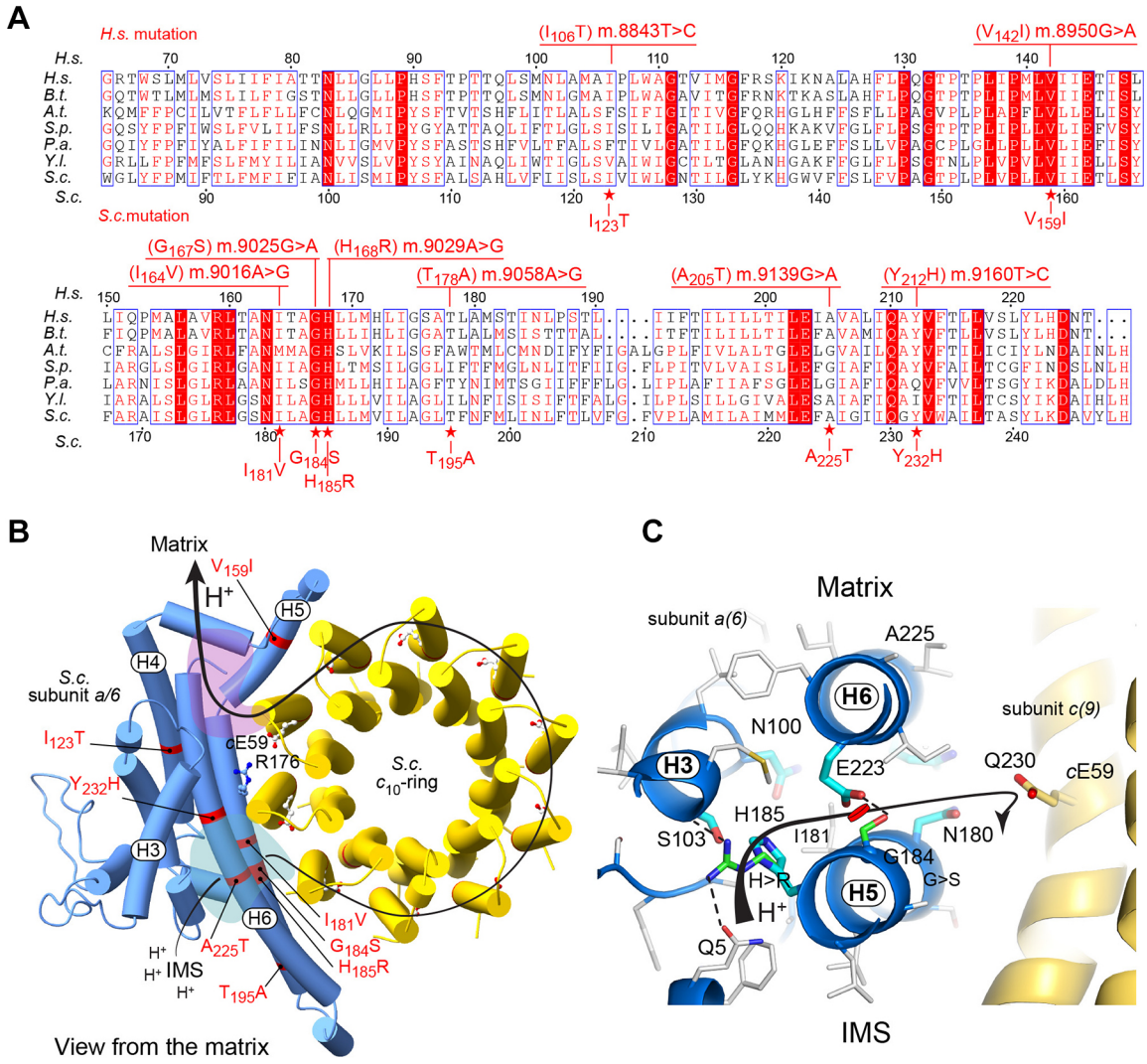

Fig. 5. Evolutionary conservation and topology of the subunit *a* residues targeted by the mutations investigated in this study. (A) Alignments of the regions of human (*H.s.*) subunit *a* in which the mutations investigated in this study are located, with their counterparts in *Bos taurus* (*B.t.*), *Arabidopsis thaliana* (*A.t.*), *Schizosaccharomyces pombe* (*S.p.*), *Podospora anserina* (*P.a.*), *Yarrowia lipolytica* (*Y.l.*) and *Saccharomyces cerevisiae* (*S.c.*). The positions of the residues in *H.s.* and *S.c.* are indicated above and below the alignments, respectively. The positions of the nucleotide changes in human mtDNA and the amino acid changes they induce, as well as the corresponding amino acid changes in the yeast protein, are indicated. (B) Overall top view from the mitochondrial matrix of the *S. cerevisiae* a/c_{10}-ring structure with the pathway along which protons are moved from the intermembrane space (IMS) to the mitochondrial matrix. The *n*-side and *p*-side hydrophilic pockets involved in this transfer are colored in purple and pale green, respectively. The E_{59} in subunit *c* and R_{176} in subunit *a* that are essential for F_O-mediated proton transfer are shown as yellow and blue sticks, respectively. The positions of the eight mutations investigated in this study are indicated. (C) Detailed view of the *p*-side pocket and the subunit *c* towards which a proton is transferred from the IMS. Important hydrophilic side chains are drawn as sticks colored in cyan. Those two amino acid changes ($G_{184}S$ and $H_{185}R$) that compromise proton translocation are drawn as sticks with their carbon in green color.

pathogenic (Lopez-Gallardo et al., 2014). The present study strongly supports this proposal. Indeed, the growth of yeast cells with an equivalent of this mutation (aH$_{185}$R) on respiratory carbon sources was less efficient than that in wild-type cells and was highly sensitive to chemical inhibition of F_O with oligomycin, indicating a substantial loss of ATP synthase function; this was confirmed by direct ATP synthesis activity measurements in isolated mitochondria. Based on previous studies in *E. coli* (Cain and Simoni, 1988; Lightowlers et al., 1988) and the results reported here, we suggest that aH$_{185}$R compromises the transport of protons from the mitochondrial intermembrane space to the *c*-ring motor of ATP synthase.

The four remaining variants here investigated were identified in patients presenting with schizophrenia (m.8843T>C, m.9160T>C), maternally inherited Leigh syndrome (MILS) (m.9025G>A) or left ventricular hypertrabeculation syndrome (LVHT) (m.9058A>G) (Table 1). Of these, only m.9025G>A had clear detrimental effects in a yeast model of this mutation (aG$_{184}$S), as evidenced by a higher *in vivo* sensitivity to oligomycin (Fig. 2A,B) and a substantial drop in the rate of mitochondrial ATP synthesis relative to that in wild-type yeast (Table 2). This variant was found in three independent patients with MILS or motor neuropathy but was also found in 13 healthy individuals, and in homoplasmy in the asymptomatic mother and sister of one of the above patients (Lopez-Gallardo et al., 2014); therefore, it was classified as benign in the ClinVar database. However, the pathogenicity score of this variant is very high (Pereira et al., 2011), and another substitution of glycine 167 – into lysine – owing to m.9026G>A was found in two members of one family with intellectual

disability, dysautonomia, headaches, myalgia and fatigue (Ganetzky et al., 2019). The p.G_{167}K substitution was proposed to be pathogenic based on fibroblast respirometry and family genetics. These findings, and the data we obtained in the yeast model, provide arguments for the pathogenicity of the m.9025G>A variant as well. As we described above, this mutation possibly prevents a glutamate residue (aE_{223}) from functioning properly in the transfer of protons within the *p*-side proton channel of F_O.

Although equivalents of m.8950G>A and m.9025G>A had significant detrimental effects in yeast, these variants were seen at homoplasmy in >40 healthy individuals in the gnomAD population database. This raises the possibility that, in those individuals showing a clinical phenotype, these variants act in synergy with some additional genetic defect in nuclear DNA, as was previously observed for other mtDNA mutations (Dunham-Snary et al., 2018; Pickett et al., 2018). Also, it is well known that some mutations in mtDNA start to compromise human health in older age. This was, for instance, observed in a patient who, at the age of 68, developed a common mitochondrial disorder due to a mutation in the *MT-ATP6* gene (J.P.d.R. and V. Procaccio, University Hospital of Angers, Angers, France, personal communication). It would be interesting to follow up those healthy individuals carrying m.8950G>A or m.9025G>A when they become aged.

The good preservation of ATP synthase function in yeast strains with equivalents of m.8843T>C ($aI_{123}T$), m.9160T>C ($aY_{232}H$) and m.9058A>G ($aT_{195}A$) suggests that these mutations do not have, at least alone, the potential to compromise human health.

Thanks to their unique features, such as the ability to fermentative growth, the possibility of mtDNA mutagenesis and its homoplasmy, yeast *S cerevisiae* is a very good model for understanding the pathogenesis of mutations in genes encoded in mtDNA. However, the usefulness of yeast is limited to highly evolutionarily conserved proteins like Atp6, but less so for Atp8, which shows great diversity at the sequence level. Although the analyses of many of the variants we have examined so far in this model correlate with the severity of the disease in patients, information on family history, and studies' on patients cells or tissues, are necessary to unequivocally classify mitochondrial variants as pathogenic.

MATERIALS AND METHODS

Media for growing yeast

The media used for growing yeast were as follows: YPGA (1% Bacto yeast extract, 1% Bacto Peptone, 2% or 10% glucose, 40 mg/l adenine), YPGalA (1% Bacto yeast extract, 1% Bacto Peptone, 2% galactose, 40 mg/l adenine), YPGlyA (1% Bacto yeast extract, 1% Bacto Peptone, 2% glycerol, 40 mg/l adenine), BIOL-Leu [1.7 g/l YNB w/o (yeast nitrogen base without amino acids), 5 g/l ammonium sulfate, 0.8 g/l CSM-Leu drop out mix, 5% glucose, 182.5 g/l sorbitol and 40 mg/l adenine]. Media were solidified by the addition of 2-5% (w/v) Bacto agar. Growth curves were established with a Bioscreen CTM system. For the drop test, cells were grown in liquid YPGA medium for one night. The density of cultures was measured, and they were serially diluted in water to have, in the fifth dilution, ten colonies in a 5 µl drop. Then, the drops were added to the plates. Growth tests were performed at least two times. For halo tests, exponentially grown cells, at an optical density at a wavelength of 600 nm (OD_{600}) of 0.05, were homogeneously spread with sterile glass beads on a Petri dish containing solid YPGlyA medium. Sterile filters were deposited on the plate and spotted with 2 µl of 10 mM oligomycin dissolved in dimethyl sulfoxide (DMSO). The diameter of the growth inhibition halo, a value permitting the comparison of strains for their sensitivity to oligomycin, was measured with the ImageJ program.

Construction of the yeast *atp6* mutants

Q5® and QuikChange II site-directed mutagenesis kits (from NEBiolabs and Agilent, respectively) were used for mutagenizing the yeast *ATP6* gene (Tribouillard-Tanvier et al., 2022). To this end, three previously described plasmids were used: pSDC8 (Zeng et al., 2007), pSDC9 (Kucharczyk et al., 2009b) and pSDC14 (Rak et al., 2007a). Plasmid pSDC8 contains, within a *Bam*HI-*Eco*RI fragment, the first 698 bp of the yeast *ATP6* gene, while the remaining 82 bp are within an *Eco*RI-*Bam*HI fragment in pSDC9, and pSDC14 results from cloning of the whole *ATP6* gene at the *Bam*HI site of plasmid pJM2 (Fig. 1). Equivalents of the m.8843T>C, m.8950G>A, m.9016A>G, m.9025G>A, m.9029A>G and m.9058A>G mutations ($atp6^{mut}$) were introduced in pSDC8, and equivalents of m.9139G>A and m.9160T>C were created in pSDC9 (see Table S1 for the sequences of the mutagenic primers and Table 1 for the corresponding codon and amino acid changes). The mutated *ATP6* fragments in pSDC8 and pSDC9 were cut off (with *Bam*HI+*Eco*RI and *Eco*RI+*Sap*I, respectively) and exchanged with the corresponding (non-mutated) fragments in pSDC14, yielding the final plasmids with the $atp6^{mut}$ mutations in the entire *ATP6* gene (pATP6^{mut}). These plasmids, together with a plasmid (Yep351) carrying the nuclear *LEU2* gene, were introduced into the ρ^0 strain DFS160 by microprojectile bombardment using a biolistic PDS-1000/He particle delivery system (Bio-Rad) as described (Bonnefoy and Fox, 2001). The Leu^+ transformants (a few hundred per plate) were cross-replicated during one night on a rich glucose medium (YPGA) with cells from strain MR10, in which the coding sequence of *ATP6* is replaced by the $ARG8^m$ genetic marker (Rak et al., 2007b). In these crosses, the Leu^+ transformants that contain the pATP6^{mut} plasmid (ρ^- $atp6^{mut}$) in their mitochondria are able, by mtDNA recombination, to replace $ARG8^m$ by the mutated *ATP6* gene, yielding strains in which the *atp6* mutation is integrated in a complete mitochondrial genome (ρ^+ $atp6^{mut}$). If the $atp6^{mut}$ does not fully inactivate the ATP synthase, the ρ^+ $atp6^{mut}$ clones can be selected by their ability to grow on glycerol medium (YPGlyA). Respiring clones were obtained with the eight pATP6^{mut} plasmids, and the presence in these clones of the $atp6^{mut}$ mutations was confirmed by DNA sequencing with primers oATP6-1 and oATP6-10 (Table S1).

Biochemical analyses of mitochondria

Mitochondria were prepared from yeast cells grown in rich galactose (YPGalA) to an OD_{600} of 4 by the enzymatic method described in the reference (Guerin et al., 1979). For respiration and ATP synthesis assays, they were diluted to 0.075 µg/ml in respiration buffer (10 mM Tris-maleate pH 6.8, 0.65 M mannitol, 0.36 mM EGTA and 5 mM Tris-phosphate). Oxygen consumption rates were measured using a Clarke electrode in the presence of 4 mM NADH (state 4 respiration), 150 µM ADP (state 3 respiration) or 4 µM CCCP (uncoupled respiration), as previously described (Rigoulet and Guerin, 1979). A higher concentration of ADP (750 µM) was used to measure the rate of ATP synthesis in the absence and presence (3 µg/ml) of oligomycin. Aliquots were taken every 15 s, and the production of ATP, after stopping the reaction with 3.5% (w/v) perchloric acid and 12.5 mM EDTA, was quantified using Kinase-Glo Max Luminescence Kinase Assay (Promega) and a Beckman Coulter's Paradigm Plate Reader. Variations in $\Delta\Psi$ were evaluated in the respiration buffer containing 0.150 mg/ml mitochondria and Rhodamine 123 (0.5 µg/ml), with an excitation wavelength of 485 nm and an emission wavelength of 533 nm under constant stirring using a Cary Eclipse Fluorescence Spectrophotometer (Agilent Technologies) (Emaus et al., 1986). BN-PAGE was performed as described (Schagger and von Jagow, 1991) from mitochondrial samples containing 200 µg of proteins suspended in 100 µl extraction buffer [30 mM HEPES pH 6.8, 150 mM potassium acetate, 12% glycerol, 2 mM 6-aminocaproic acid, 1 mM EGTA, 1.5% digitonin (Sigma-Aldrich)]. To avoid protein degradation, one protease inhibitor cocktail tablet (Roche) per 10 ml and 1 mM PMSF were added to the samples. After 26 min incubation on ice, the extracts were cleared by centrifugation (21,950 ***g***, 4°C, 30 min), supplemented with 4.5 µl loading dye (5% Serva Blue G-250, 750 mM 6-aminocaproic acid) and run on NativePAGE™ 3-12% Bis-Tris Gels (Thermo Fisher Scientific). After transfer onto a PVDF membrane, ATP synthase complexes were detected using polyclonal antibodies against yeast subunit β (Atp2p) or *a* (Atp6p) at a 1:10,000 dilution. For sodium dodecyl-sulfate (SDS)-PAGE analysis, 10 OD_{600} of overnight grown cells in YPGalA medium was centrifuged and suspended in 500 µl of 0.2 M NaOH. After 10 min incubation on ice, the samples were mixed with 50 µl of 50% trichloroacetic acid, incubated for 10 min on ice, and centrifuged at 21,950 ***g*** for 10 min at 4°C. The protein pellet was

washed with 1 ml of 1 M Tris-base and suspended in 50 µl of 5% SDS, and the concentration of proteins was measured by the method of Lowry (Lowry et al., 1951). For those samples prepared from cells grown at 28°C or 36°C, 40 µg and 75 µg of proteins, respectively, were run on 12% SDS-PAGE gels (Laemmli, 1970). The proteins were then transferred onto a nitrocellulose membrane using an iBlot2 Gel Transfer Device from Thermo Fisher Scientific and analyzed by western blotting using antibodies against Atp2, Atp6, Atp7 and Por1 [these were kindly provided by Marie-France Giraud (Institut de Biochimie et Génétique Cellulaires, Centre National de la Recherche Scientifique, France; 1:10,000) and Teresa Żołądek (Institute of Biochemistry and Biophysics, Polish Academy of Sciences, Warsaw, Poland; 1:10,000)].

Amino acid alignments and topology of subunit *a* mutations

Multiple sequences of ATP synthase *a*-subunits of various origins were aligned and drawn using Clustal Omega (Sievers et al., 2011) and Espript 3.0 (Robert and Gouet, 2014), respectively. Molecular views of subunit *a* and *c*10-ring were obtained from the dimeric Fo domain of *S. cerevisiae* ATP synthase [PDB ID: 6b2z (Guo et al., 2017)]. The structure figure was drawn using PyMOL molecular graphic system.

Statistical analysis

At least three biological and three technical replicates were performed for all experiments. Unpaired two-tailed Student's *t*-test was used for all datasets. Significance and confidence level was set at 0.05.

Statement of ethics

The permission number for work with genetically modified microorganisms (GMM I) for R.K. is 01.2-28/201.

Acknowledgements

The authors thank Dr Agnieszka Szczepankowska for help working with the Bioscreen CTM system.

Competing interests

The authors declare no competing or financial interests.

Author contributions

Conceptualization: R.K.; Validation: C.C., J.-P.d.R.; Investigation: E.B., K.N., C.P., C.C., A.D., J.P.; Data curation: E.B., K.N., C.P., J.P.; Writing - original draft: R.K., E.B., K.N., A.D.; Writing - review & editing: R.K., J.-P.d.R., D.T.-T.; Visualization: A.D.; Supervision: R.K.; Funding acquisition: R.K., D.T.-T.

Funding

This work was supported by Narodowe Centrum Nauki (2016/23/B/NZ3/02098 to R.K.) and Association Française contre les Myopathies (22382 to D.T.-T.). Open Access funding provided by Polska Akademia Nauk. Deposited in PMC for immediate release.

Data availability

All relevant data can be found within the article and its supplementary information.

References

Abu-Amero, K. K. and Bosley, T. M. (2005). Detection of mitochondrial respiratory dysfunction in circulating lymphocytes using resazurin. *Arch. Pathol. Lab. Med.* **129**, 1295-1298. doi:10.5858/2005-129-1295-DOMRDI

Al-Kafaji, G., Bakheit, H. F., Alali, F., Fattah, M., Alhajeri, S., Alharbi, M. A., Daif, A., Alsabbagh, M. M., Alwehaidah, M. S. and Bakhiet, M. (2022). Next-generation sequencing of the whole mitochondrial genome identifies functionally deleterious mutations in patients with multiple sclerosis. *PLoS One* **17**, e0263606. doi:10.1371/journal.pone.0263606

Ban, M., Elson, J., Walton, A., Turnbull, D., Compston, A., Chinnery, P. and Sawcer, S. (2008). Investigation of the role of mitochondrial DNA in multiple sclerosis susceptibility. *PLoS One* **3**, e2891. doi:10.1371/journal.pone.0002891

Berry, E. A., Guergova-Kuras, M., Huang, L. S. and Crofts, A. R. (2000). Structure and function of cytochrome *bc* complexes. *Annu. Rev. Biochem.* **69**, 1005-1075. doi:10.1146/annurev.biochem.69.1.1005

Bonnefoy, N. and Fox, T. D. (2001). Genetic transformation of Saccharomyces cerevisiae mitochondria. *Methods Cell Biol.* **65**, 381-396. doi:10.1016/S0091-679X(01)65022-2

Brautbar, A., Wang, J., Abdenur, J. E., Chang, R. C., Thomas, J. A., Grebe, T. A., Lim, C., Weng, S. W., Graham, B. H. and Wong, L. J. (2008). The mitochondrial 13513G>A mutation is associated with Leigh disease phenotypes independent of complex I deficiency in muscle. *Mol. Genet. Metab.* **94**, 485-490. doi:10.1016/j.ymgme.2008.04.004

Cain, B. D. and Simoni, R. D. (1988). Interaction between Glu-219 and His-245 within the a subunit of F1F0-ATPase in Escherichia coli. *J. Biol. Chem.* **263**, 6606-6612. doi:10.1016/S0021-9258(18)68684-3

Cho, S. I., Lee, S., Mok, Y. G., Lim, K., Lee, J., Lee, J. M., Chung, E. and Kim, J. S. (2022). Targeted A-to-G base editing in human mitochondrial DNA with programmable deaminases. *Cell* **185**, 1764-1776.e12. doi:10.1016/j.cell.2022.03.039

Dautant, A., Meier, T., Hahn, A., Tribouillard-Tanvier, D., Di Rago, J. P. and Kucharczyk, R. (2018). ATP synthase diseases of mitochondrial genetic origin. *Front. Physiol.* **9**, 329. doi:10.3389/fphys.2018.00329

Ding, Q., Kucharczyk, R., Zhao, W., Dautant, A., Xu, S., Niedzwiecka, K., Su, X., Giraud, M. F., Gombeau, K., Zhang, M. et al. (2020). Case report: identification of a novel variant (m.8909T>C) of human mitochondrial ATP6 gene and its functional consequences on yeast ATP synthase. *Life (Basel)* **10**, 215. doi:10.3390/life10090215

Dunham-Snary, K. J., Sandel, M. W., Sammy, M. J., Westbrook, D. G., Xiao, R., Mcmonigle, R. J., Ratcliffe, W. F., Penn, A., Young, M. E. and Ballinger, S. W. (2018). Mitochondrial - nuclear genetic interaction modulates whole body metabolism, adiposity and gene expression in vivo. *EBioMedicine* **36**, 316-328. doi:10.1016/j.ebiom.2018.08.036

Duvezin-Caubet, S., Rak, M., Lefebvre-Legendre, L., Tetaud, E., Bonnefoy, N. and di Rago, J. P. (2006). A "petite obligate" mutant of *Saccharomyces cerevisiae*: functional mtDNA is lethal in cells lacking the delta subunit of mitochondrial F1-ATPase. *J. Biol. Chem.* **281**, 16305-16313. doi:10.1074/jbc.M513805200

El-Hattab, A. W., Emrick, L. T., Hsu, J. W., Chanprasert, S., Jahoor, F., Scaglia, F. and Craigen, W. J. (2014). Glucose metabolism derangements in adults with the MELAS m.3243A>G mutation. *Mitochondrion* **18**, 63-69. doi:10.1016/j.mito.2014.07.008

Emaus, R. K., Grunwald, R. and Lemasters, J. J. (1986). Rhodamine 123 as a probe of transmembrane potential in isolated rat-liver mitochondria: spectral and metabolic properties. *Biochim. Biophys. Acta* **850**, 436-448. doi:10.1016/0005-2728(86)90112-X

Finsterer, J., Mancuso, M., Pareyson, D., Burgunder, J. M. and Klopstock, T. (2018). Mitochondrial disorders of the retinal ganglion cells and the optic nerve. *Mitochondrion* **42**, 1-10. doi:10.1016/j.mito.2017.10.003

Ganetzky, R. D., Stendel, C., Mccormick, E. M., Zolkipli-Cunningham, Z., Goldstein, A. C., Klopstock, T. and Falk, M. J. (2019). MT-ATP6 mitochondrial disease variants: Phenotypic and biochemical features analysis in 218 published cases and cohort of 14 new cases. *Hum. Mutat.* **40**, 499-515. doi:10.1002/humu.23723

Gorman, G. S., Chinnery, P. F., Dimauro, S., Hirano, M., Koga, Y., Mcfarland, R., Suomalainen, A., Thorburn, D. R., Zeviani, M. and Turnbull, D. M. (2016). Mitochondrial diseases. *Nat. Rev. Dis. Primers* **2**, 16080. doi:10.1038/nrdp.2016.80

Guerin, B., Labbe, P. and Somlo, M. (1979). Preparation of yeast mitochondria (Saccharomyces cerevisiae) with good P/O and respiratory control ratios. *Methods Enzymol.* **55**, 149-159. doi:10.1016/0076-6879(79)55021-6

Guo, H., Bueler, S. A. and Rubinstein, J. L. (2017). Atomic model for the dimeric FO region of mitochondrial ATP synthase. *Science* **358**, 936-940. doi:10.1126/science.aao4815

Hahn, A., Parey, K., Bublitz, M., Mills, D. J., Zickermann, V., Vonck, J., Kuhlbrandt, W. and Meier, T. (2016). Structure of a complete ATP synthase dimer reveals the molecular basis of inner mitochondrial membrane morphology. *Mol. Cell* **63**, 445-456. doi:10.1016/j.molcel.2016.05.037

Hinkle, P. C. (2005). P/O ratios of mitochondrial oxidative phosphorylation. *Biochim. Biophys. Acta.* **1706**, 1-11. doi:10.1016/j.bbabio.2004.09.004

Holt, I. J., Harding, A. E., Petty, R. K. and Morgan-Hughes, J. A. (1990). A new mitochondrial disease associated with mitochondrial DNA heteroplasmy. *Am. J. Hum. Genet.* **46**, 428-433.

Hudson, G., Gomez-Duran, A., Wilson, I. J. and Chinnery, P. F. (2014). Recent mitochondrial DNA mutations increase the risk of developing common late-onset human diseases. *PLoS Genet.* **10**, e1004369. doi:10.1371/journal.pgen.1004369

Ju, Y. S., Alexandrov, L. B., Gerstung, M., Martincorena, I., Nik-Zainal, S., Ramakrishna, M., Davies, H. R., Papaemmanuil, E., Gundem, G., Shlien, A. et al. (2014). Origins and functional consequences of somatic mitochondrial DNA mutations in human cancer. *Elife* **3**, e02935. doi:10.7554/eLife.02935

Kabala, A. M., Lasserre, J. P., Ackerman, S. H., Di Rago, J. P. and Kucharczyk, R. (2014). Defining the impact on yeast ATP synthase of two pathogenic human mitochondrial DNA mutations, T9185C and T9191C. *Biochimie* **100**, 200-206. doi:10.1016/j.biochi.2013.11.024

Kucharczyk, R., Rak, M. and Di Rago, J. P. (2009a). Biochemical consequences in yeast of the human mitochondrial DNA 8993T>C mutation in the ATPase6 gene found in NARP/MILS patients. *Biochim. Biophys. Acta* **1793**, 817-824. doi:10.1016/j.bbamcr.2009.02.011

Kucharczyk, R., Salin, B. and Di Rago, J. P. (2009b). Introducing the human Leigh syndrome mutation T9176G into Saccharomyces cerevisiae mitochondrial DNA leads to severe defects in the incorporation of Atp6p into the ATP synthase and in the mitochondrial morphology. *Hum. Mol. Genet.* **18**, 2889-2898. doi:10.1093/hmg/ddp226

Kucharczyk, R., Zick, M., Bietenhader, M., Rak, M., Couplan, E., Blondel, M., Caubet, S. D. and Di Rago, J. P. (2009c). Mitochondrial ATP synthase disorders: molecular mechanisms and the quest for curative therapeutic approaches. *Biochim. Biophys. Acta* **1793**, 186-199. doi:10.1016/j.bbamcr.2008.06.012

Kucharczyk, R., Ezkurdia, N., Couplan, E., Procaccio, V., Ackerman, S. H., Blondel, M. and Di Rago, J. P. (2010). Consequences of the pathogenic T9176C mutation of human mitochondrial DNA on yeast mitochondrial ATP synthase. *Biochim. Biophys. Acta* **1797**, 1105-1112. doi:10.1016/j.bbabio.2009.12.022

Kucharczyk, R., Giraud, M. F., Brethes, D., Wysocka-Kapcinska, M., Ezkurdia, N., Salin, B., Velours, J., Camougrand, N., Haraux, F. and Di Rago, J. P. (2013). Defining the pathogenesis of human mtDNA mutations using a yeast model: the case of T8851C. *Int. J. Biochem. Cell Biol.* **45**, 130-140. doi:10.1016/j.biocel.2012.07.001

Kucharczyk, R., Dautant, A., Godard, F., Tribouillard-Tanvier, D. and Di Rago, J. P. (2019a). Functional investigation of an universally conserved leucine residue in subunit a of ATP synthase targeted by the pathogenic m.9176T>G mutation. *Biochim. Biophys. Acta Bioenerg.* **1860**, 52-59. doi:10.1016/j.bbabio.2018.11.005

Kucharczyk, R., Dautant, A., Gombeau, K., Godard, F., Tribouillard-Tanvier, D. and Di Rago, J. P. (2019b). The pathogenic MT-ATP6 m.8851T>C mutation prevents proton movements within the n-side hydrophilic cleft of the membrane domain of ATP synthase. *Biochim. Biophys. Acta Bioenerg.* **1860**, 562-572. doi:10.1016/j.bbabio.2019.06.002

La Morgia, C., Achilli, A., Iommarini, L., Barboni, P., Pala, M., Olivieri, A., Zanna, C., Vidoni, S., Tonon, C., Lodi, R. et al. (2008). Rare mtDNA variants in Leber hereditary optic neuropathy families with recurrence of myoclonus. *Neurology* **70**, 762-770. doi:10.1212/01.wnl.0000295505.74234.d0

Laemmli, U. K. (1970). Cleavage of structural proteins during the assembly of the head of bacteriophage T4. *Nature* **227**, 680-685. doi:10.1038/227680a0

Lei, Z., Meng, H., Liu, L., Zhao, H., Rao, X., Yan, Y., Wu, H., Liu, M., He, A. and Yi, C. (2022). Mitochondrial base editor induces substantial nuclear off-target mutations. *Nature* **606**, 804-811. doi:10.1038/s41586-022-04836-5

Lightowlers, R. N., Howitt, S. M., Hatch, L., Gibson, F. and Cox, G. (1988). The proton pore in the Escherichia coli F0F1-ATPase: substitution of glutamate by glutamine at position 219 of the alpha-subunit prevents F0-mediated proton permeability. *Biochim. Biophys. Acta* **933**, 241-248. doi:10.1016/0005-2728(88)90031-X

Lopez-Gallardo, E., Emperador, S., Solano, A., Llobet, L., Martin-Navarro, A., Lopez-Perez, M. J., Briones, P., Pineda, M., Artuch, R., Barraquer, E. et al. (2014). Expanding the clinical phenotypes of MT-ATP6 mutations. *Hum. Mol. Genet.* **23**, 6191-6200. doi:10.1093/hmg/ddu339

Lowry, O. H., Rosebrough, N. J., Farr, A. L. and Randall, R. J. (1951). Protein measurement with the Folin phenol reagent. *J. Biol. Chem.* **193**, 265-275. doi:10.1016/S0021-9258(19)52451-6

Mcmanus, M. J., Picard, M., Chen, H. W., De Haas, H. J., Potluri, P., Leipzig, J., Towheed, A., Angelin, A., Sengupta, P., Morrow, R. M. et al. (2019). Mitochondrial DNA variation dictates expressivity and progression of nuclear DNA mutations causing cardiomyopathy. *Cell Metab.* **29**, 78-90.e5. doi:10.1016/j.cmet.2018.08.002

Michel, H. (1998). The mechanism of proton pumping by cytochrome *c* oxidase. *Proc. Natl. Acad. Sci. U S A* **95**, 12819-12824. doi:10.1073/pnas.95.22.12819

Mok, B. Y., De Moraes, M. H., Zeng, J., Bosch, D. E., Kotrys, A. V., Raguram, A., Hsu, F., Radey, M. C., Peterson, S. B., Mootha, V. K. et al. (2020). A bacterial cytidine deaminase toxin enables CRISPR-free mitochondrial base editing. *Nature* **583**, 631-637. doi:10.1038/s41586-020-2477-4

Mukhopadhyay, A., Uh, M. and Mueller, D. M. (1994). Level of ATP synthase activity required for yeast Saccharomyces cerevisiae to grow on glycerol media. *FEBS Lett.* **343**, 160-164. doi:10.1016/0014-5793(94)80310-2

Pereira, L., Soares, P., Radivojac, P., Li, B. and Samuels, D. C. (2011). Comparing phylogeny and the predicted pathogenicity of protein variations reveals equal purifying selection across the global human mtDNA diversity. *Am. J. Hum. Genet.* **88**, 433-439. doi:10.1016/j.ajhg.2011.03.006

Pfeffer, G. and Chinnery, P. F. (2013). Diagnosis and treatment of mitochondrial myopathies. *Ann. Med.* **45**, 4-16. doi:10.3109/07853890.2011.605389

Pickett, S. J., Grady, J. P., Ng, Y. S., Gorman, G. S., Schaefer, A. M., Wilson, I. J., Cordell, H. J., Turnbull, D. M., Taylor, R. W. and Mcfarland, R. (2018). Phenotypic heterogeneity in m.3243A>G mitochondrial disease: The role of nuclear factors. *Ann. Clin. Transl. Neurol.* **5**, 333-345. doi:10.1002/acn3.532

Povalko, N., Zakharova, E., Rudenskaia, G., Akita, Y., Hirata, K., Toyojiro, M. and Koga, Y. (2005). A new sequence variant in mitochondrial DNA associated with high penetrance of Russian Leber hereditary optic neuropathy. *Mitochondrion* **5**, 194-199. doi:10.1016/j.mito.2005.03.003

Rak, M., Tetaud, E., Duvezin-Caubet, S., Ezkurdia, N., Bietenhader, M., Rytka, J. and Di Rago, J. P. (2007a). A yeast model of the neurogenic ataxia retinitis pigmentosa (NARP) T8993G mutation in the mitochondrial ATP synthase-6 gene. *J. Biol. Chem.* **282**, 34039-34047. doi:10.1074/jbc.M703053200

Rak, M., Tetaud, E., Godard, F., Sagot, I., Salin, B., Duvezin-Caubet, S., Slonimski, P. P., Rytka, J. and Di Rago, J. P. (2007b). Yeast cells lacking the mitochondrial gene encoding the ATP synthase subunit 6 exhibit a selective loss of complex IV and unusual mitochondrial morphology. *J. Biol. Chem.* **282**, 10853-10864. doi:10.1074/jbc.M608692200

Rigoulet, M. and Guerin, B. (1979). Phosphate transport and ATP synthesis in yeast mitochondria: effect of a new inhibitor: the tribenzylphosphate. *FEBS Lett.* **102**, 18-22. doi:10.1016/0014-5793(79)80919-9

Robert, X. and Gouet, P. (2014). Deciphering key features in protein structures with the new ENDscript server. *Nucleic Acids Res.* **42**, W320-W324. doi:10.1093/nar/gku316

Saraste, M. (1999). Oxidative phosphorylation at the fin de siècle. *Science* **283**, 1488-1493. doi:10.1126/science.283.5407.1488

Schagger, H. and Von Jagow, G. (1991). Blue native electrophoresis for isolation of membrane protein complexes in enzymatically active form. *Anal. Biochem.* **199**, 223-231. doi:10.1016/0003-2697(91)90094-A

Schultz, B. E. and Chan, S. I. (2001). Structures and proton-pumping strategies of mitochondrial respiratory enzymes. *Annu. Rev. Biophys. Biomol. Struct.* **30**, 23-65. doi:10.1146/annurev.biophys.30.1.23

Sequeira, A., Rollins, B., Magnan, C., Van Oven, M., Baldi, P., Myers, R. M., Barchas, J. D., Schatzberg, A. F., Watson, S. J., Akil, H. et al. (2015). Mitochondrial mutations in subjects with psychiatric disorders. *PLoS One* **10**, e0127280. doi:10.1371/journal.pone.0127280

Sievers, F., Wilm, A., Dineen, D., Gibson, T. J., Karplus, K., Li, W., Lopez, R., Mcwilliam, H., Remmert, M., Soding, J. et al. (2011). Fast, scalable generation of high-quality protein multiple sequence alignments using Clustal Omega. *Mol. Syst. Biol.* **7**, 539. doi:10.1038/msb.2011.75

Skoczen, N., Dautant, A., Binko, K., Godard, F., Bouhier, M., Su, X., Lasserre, J. P., Giraud, M. F., Tribouillard-Tanvier, D., Chen, H. et al. (2018). Molecular basis of diseases caused by the mtDNA mutation m.8969G>A in the subunit a of ATP synthase. *Biochim. Biophys. Acta Bioenerg.* **1859**, 602-611. doi:10.1016/j.bbabio.2018.05.009

Sobti, M., Walshe, J. L., Wu, D., Ishmukhametov, R., Zeng, Y. C., Robinson, C. V., Berry, R. M. and Stewart, A. G. (2020). Cryo-EM structures provide insight into how E. coli F1Fo ATP synthase accommodates symmetry mismatch. *Nat. Commun.* **11**, 2615. doi:10.1038/s41467-020-16387-2

Spikes, T. E., Montgomery, M. G. and Walker, J. E. (2020). Structure of the dimeric ATP synthase from bovine mitochondria. *Proc. Natl. Acad. Sci. USA* **117**, 23519-23526. doi:10.1073/pnas.2013998117

Srivastava, A. P., Luo, M., Zhou, W., Symersky, J., Bai, D., Chambers, M. G., Faraldo-Gomez, J. D., Liao, M. and Mueller, D. M. (2018). High-resolution cryo-EM analysis of the yeast ATP synthase in a lipid membrane. *Science* **360**, eaas9699. doi:10.1126/science.aas969

Steele, D. F., Butler, C. A. and Fox, T. D. (1996). Expression of a recoded nuclear gene inserted into yeast mitochondrial DNA is limited by mRNA-specific translational activation. *Proc. Natl. Acad. Sci. USA* **93**, 5253-5257. doi:10.1073/pnas.93.11.5253

Su, X., Dautant, A., Godard, F., Bouhier, M., Zoladek, T., Kucharczyk, R., Di Rago, J. P. and Tribouillard-Tanvier, D. (2020). Molecular basis of the pathogenic mechanism induced by the m.9191T>C mutation in mitochondrial ATP6 gene. *Int. J. Mol. Sci.* **21**, 5083. doi:10.3390/ijms21145083

Su, X., Dautant, A., Rak, M., Godard, F., Ezkurdia, N., Bouhier, M., Bietenhader, M., Mueller, D. M., Kucharczyk, R., Di Rago, J. P. et al. (2021). The pathogenic m.8993 T>G mutation in mitochondrial ATP6 gene prevents proton release from the subunit c-ring rotor of ATP synthase. *Hum. Mol. Genet.* **30**, 381-392. doi:10.1093/hmg/ddab043

Tang, S., Batra, A., Zhang, Y., Ebenroth, E. S. and Huang, T. (2010). Left ventricular noncompaction is associated with mutations in the mitochondrial genome. *Mitochondrion* **10**, 350-357. doi:10.1016/j.mito.2010.02.003

Tribouillard-Tanvier, D., Dautant, A., Godard, F., Charles, C., Panja, C., Di Rago, J. P. and Kucharczyk, R. (2022). Creation of yeast models for evaluating the pathogenicity of mutations in the human mitochondrial gene MT-ATP6 and discovering therapeutic molecules. *Methods Mol. Biol.* **2497**, 221-242. doi:10.1007/978-1-0716-2309-1_14

Ueno, H., Nishigaki, Y., Kong, Q. P., Fuku, N., Kojima, S., Iwata, N., Ozaki, N. and Tanaka, M. (2009). Analysis of mitochondrial DNA variants in Japanese patients with schizophrenia. *Mitochondrion* **9**, 385-393. doi:10.1016/j.mito.2009.06.003

Venard, R., Brethes, D., Giraud, M. F., Vaillier, J., Velours, J. and Haraux, F. (2003). Investigation of the role and mechanism of IF1 and STF1 proteins, twin inhibitory peptides which interact with the yeast mitochondrial ATP synthase. *Biochemistry* **42**, 7626-7636. doi:10.1021/bi034394t

Wallace, D. C. (2010). Mitochondrial DNA mutations in disease and aging. *Environ. Mol. Mutagen.* **51**, 440-450. doi:10.1002/em.20586

Wang, J., Balciuniene, J., Diaz-Miranda, M. A., Mccormick, E. M., Aref-Eshghi, E., Muir, A. M., Cao, K., Troiani, J., Moseley, A., Fan, Z. et al. (2022). Advanced approach for comprehensive mtDNA genome testing in mitochondrial disease. *Mol. Genet. Metab.* **135**, 93-101. doi:10.1016/j.ymgme.2021.12.006

Wilkins, H. M., Carl, S. M. and Swerdlow, R. H. (2014). Cytoplasmic hybrid (cybrid) cell lines as a practical model for mitochondriopathies. *Redox Biol.* **2**, 619-631. doi:10.1016/j.redox.2014.03.006

Yamamura, M., Nagami, Y., Vongsuvanlert, V., Kumnuanta, J. and Kamihara, T. (1988). Effects of elevated temperature on growth, respiratory-deficient mutation, respiratory activity, and ethanol production in yeast. *Can. J. Microbiol.* **34**, 1014-1017. doi:10.1139/m88-178

Zeng, X., Kucharczyk, R., Di Rago, J. P. and Tzagoloff, A. (2007). The leader peptide of yeast Atp6p is required for efficient interaction with the Atp9p ring of the mitochondrial ATPase. *J. Biol. Chem.* **282**, 36167-36176. doi:10.1074/jbc.M705436200

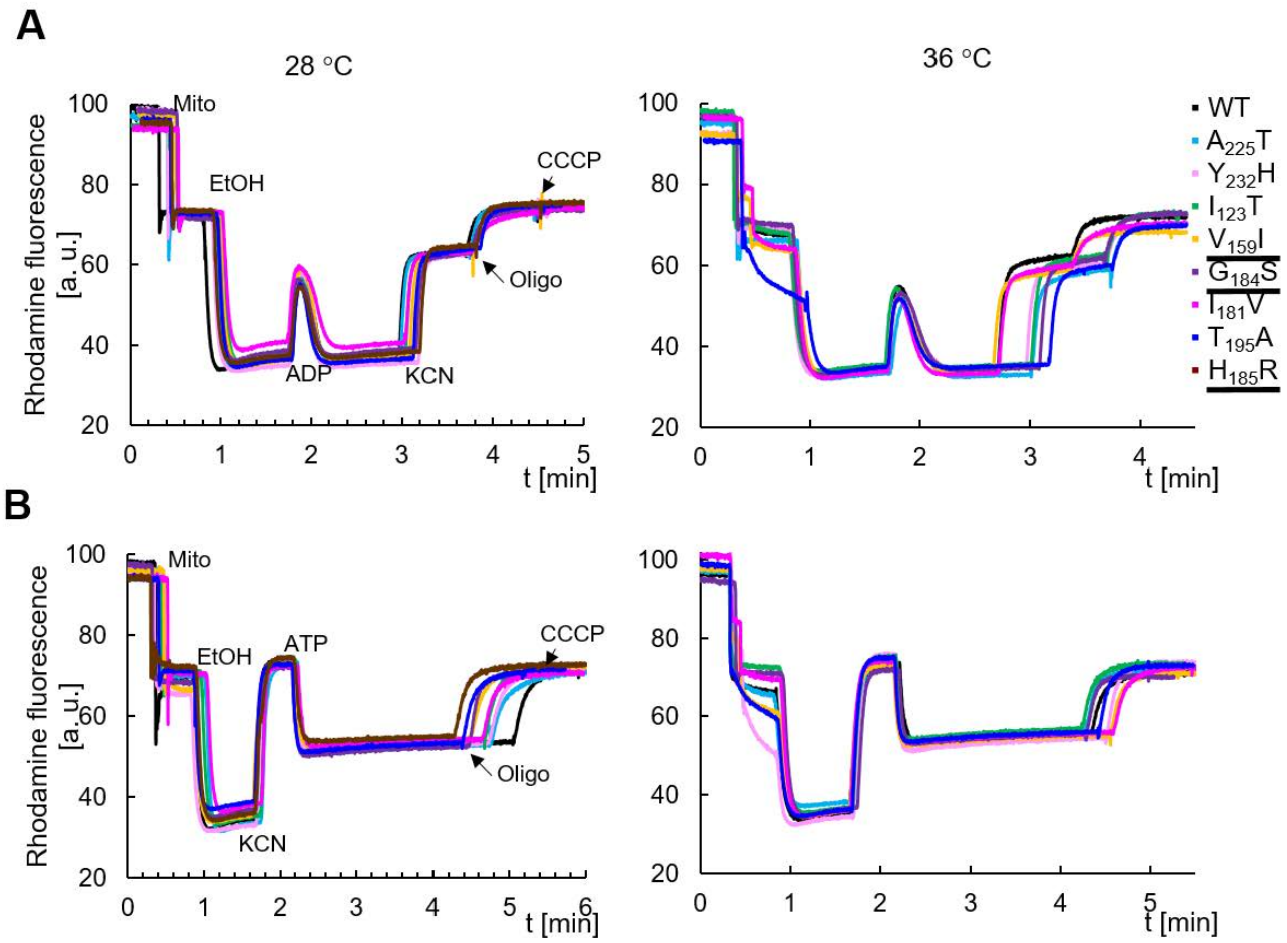

Fig. S1. Variations in mitochondrial membrane potential. The tracings in panel A show how the mitochondria responded to externally added ADP, those in panel B reflect ATP-driven proton pumping by ATP synthase. The additions were 0.5 µg/ml Rhodamine 123, 75 µg/m mitochondrial proteins (Mito), 10 µL ethanol (EtOH), 75 µM ADP, 0.2 mM ATP, 2 mM potassium cyanide (KCN), 4 µg/ml oligomycin (oligo), and 4 µM carbonyl cyanide-m-chlorophenyl hydrazone (CCCP). The shown tracings are representative of three biological repetitions.

Table S1. List of oligonucleotides used in the study (in bold are the mutagenic nucleotides)

Amino acid change in Atp6p	Codon change in *ATP6* gene	Primers		pSDC14 based plasmid	pATP6^{mut} plasmid
$I_{123}T$	ATT>ACT	For	GTATGATTCCATACTCATTTGCATTATCAGCT	pM6.1	pEB12
		Rev	CTAAAATAGTATTACCTAATCAAATAACA**G**TACTTAAAGAGATAATAAATACTAAATG		
$V_{159}I$	GTT>ATT	For	GTATTCTTCTCATTATTCGTACCTGCTGGTA	pN6.1	pEB13
		Rev	GCGAAATAAGATAAAGTTTCAATAATAA**T**TAATAAAGGTACTAATGGTAATGGTG		
$I_{181}V$	ATC>GTC	For	GAAACTTTATCTTATTTCGCTAGAGCTATTT	pO73.1	pEB20
		Rev	ATAACCATTAATAAATGACCAGCTAAGA**C**ATTAGAACCTAATCTTAAACCTAATG		
$G_{184}S$	GGT>AGT	For	CTTATTTCGCTAGAGCTATTTCATTAGGTT	pP5.1	pEB14
		Rev	CCAGCTAAAATAACCATTAATAAATGAC**T**AGCTAAGATATTAGAACCTAATCTTA		
$H_{185}R$	CAT>AGA	For	CTTATTTCGCTAGAGCTATTTCATTAGGTTTAA	pQ53.9	pEB21
		Rev	GTAAACCAGCTAAAATAACCATTAATAA**TCT**ACCAGCTAAGATATTAGAACCTAATC		
$T_{195}A$	CTA>GCA	For	TATTAATGGTTATTTTAGCTGGTTTA**GC**ATTTAATTTTATGTTAATTAATTTATTTAC	pT4.1	pEB17
		Rev	CATAGCTAAAGGTACAAAACCGAATACTAAA		
$A_{225}T$	GCT>ACT	For	CACGACGTTGTAAAACGACGGCCAGTGAATTC**A**CTATTGGTATCATTCAGGGATATGTCTG	-	pEB10
		Rev	CAGACATATCCCTGAATGATACCAATAG**T**GAATTCACTGGCCGTCGTTTTACAACGTCGTG		
$Y_{232}H$	TAT>CAT	For	GAATTCGCTATTGGTATCATTCAGGGA**C**ATGTCTGGGCTATTTTAACAGCATCATA	-	pEB11
		Rev	TATGATGCTGTTAAAATAGCCCAGACAT**G**TCCCTGAATGATACCAATAGCGAATTC		
oATP6-1	-	-	TAATATACGGGGGTGGGTCCCTCAC	-	-
oATP6-10	-	-	GGGCCGAACTCCGAAGGAGTAAG	-	-

Table S2. Genotypes and sources of yeast strains

Strain	Nuclear genotype	mtDNA	Source
DFS160	*MATα leu2Δ ura3-52 ade2-101 arg8::URA3 kar1-1*	ρ^0	Steele et al., 1996
NB40-3C	*MAT**a** lys2 leu2-3,112 ura3-52 his3ΔHinDIII arg8::HIS3*	ρ^+ *cox2-62*	Steele et al., 1996
MR6	*MAT**a** ade2-1 his3-11,15 trp1-1 leu2-3,112 ura3-1 arg8::HIS3*	ρ^+	Rak et al., 2007b
MR10	*MAT**a** ade2-1 his3-11,15 trp1-1 leu2-3,112 ura3-1 arg8::HIS3*	ρ^+*atp6::ARG8*^{m}	Rak et al., 2007b
SDC30	*MATα leu2Δ ura3-52 ade2-101 arg8::URA3 kar1-1*	ρ^- *ATP6 COX2*	Rak et al., 2007a
EBY1a	*MATα leu2Δ ura3-52 ade2-101 arg8::URA3 kar1-1*	ρ^- *atp6*-A225T	This study
EBY2a	*MATα leu2Δ ura3-52 ade2-101 arg8::URA3 kar1-1*	ρ^- *atp6*-Y232H	This study
EBY3a	*MATα leu2Δ ura3-52 ade2-101 arg8::URA3 kar1-1*	ρ^- *atp6*-I123T	This study
EBY4a	*MATα leu2Δ ura3-52 ade2-101 arg8::URA3 kar1-1*	ρ^- *atp6*-V1569I	This study
EBY5a	*MATα leu2Δ ura3-52 ade2-101 arg8::URA3 kar1-1*	ρ^- *atp6*-G184S	This study
EBY8a	*MATα leu2Δ ura3-52 ade2-101 arg8::URA3 kar1-1*	ρ^- *atp6*-I181V	This study
EBY11a	*MATα leu2Δ ura3-52 ade2-101 arg8::URA3 kar1-1*	ρ^- *atp6*-T195A	This study
EBY12a	*MATα leu2Δ ura3-52 ade2-101 arg8::URA3 kar1-1*	ρ^- *atp6*-H185R	This study
EBY1	*MAT**a** ade2-1 his3-11,15 trp1-1 leu2-3,112 ura3-1 arg8::HIS3*	ρ^+ *atp6*-A225T	This study

Strain	Nuclear genotype	mtDNA	Source
EBY2	*MAT**a** ade2-1 his3-11,15 trp1-1 leu2-3,112 ura3-1 arg8::HIS3*	ρ^+ *atp6*-Y232H	This study
EBY3	*MAT**a** ade2-1 his3-11,15 trp1-1 leu2-3,112 ura3-1 arg8::HIS3*	ρ^+ *atp6*-I123T	This study
EBY4	*MAT**a** ade2-1 his3-11,15 trp1-1 leu2-3,112 ura3-1 arg8::HIS3*	ρ^+ *atp6*-V159I	This study
EBY5	*MAT**a** ade2-1 his3-11,15 trp1-1 leu2-3,112 ura3-1 arg8::HIS3*	ρ^+*atp6*-G184S	This study
EBY8	*MAT**a** ade2-1 his3-11,15 trp1-1 leu2-3,112 ura3-1 arg8::HIS3*	ρ^+ *atp6*-I181V	This study
EBY11	*MAT**a** ade2-1 his3-11,15 trp1-1 leu2-3,112 ura3-1 arg8::HIS3*	ρ^+ *atp6*-T195A	This study
EBY12	*MAT**a** ade2-1 his3-11,15 trp1-1 leu2-3,112 ura3-1 arg8::HIS3*	ρ^+*atp6*-H185R	This study